X-RAY SPECTROMETRY
X-Ray Spectrom. **28**, 497–502 (1999)

Calculation of B K–V X-Ray Emission Spectra of Boron Nitrides

Takahiro Kaneyoshi,[1]* Hidenori Kohzuki,[2] Yasuji Muramatsu,[3] Yoshiyuki Kowada,[4] Jun Kawai[5] and Muneyuki Motoyama[2]

[1] Hyogo Prefectural Institute of Industrial Research, Kouto, Kamigori-cho, Ako-gun, Hyogo 678-1205, Japan
[2] Hyogo Prefectural Institute of Industrial Research, Suma-ku, Kobe 654-0037, Japan
[3] NTT Lifestyle and Environmental Technology Laboratories, Midori-cho, Musashino-shi, Tokyo 180-8585, Japan
[4] Hyogo University of Teacher Education, Yashiro-cho, Kato-gun, Hyogo 673-1494, Japan
[5] Department of Materials Science and Engineering, Kyoto University, Sakyo-ku, Kyoto 606-8501, Japan

The DV-Xα molecular orbital (MO) calculation method was applied to the B K–V x-ray emission spectra of hexagonal (*h*-), cubic (*c*-) and wurtzite (*w*-) type boron nitrides (BN). The calculated B 2p density of states (DOS) was in good agreement with the B K–V x-ray emission. The main peaks and low-energy satellite peaks in the B K–V x-ray emission spectra are due to the B 2p and the B 2p hybridized with N 2s, respectively. The high-energy satellite peak in the B K–V x-ray emission spectra clearly corresponds to the π^* sub-band of the B 2p DOS in *h*-BN. However, the high-energy satellite peak observed in *w*-BN is not in agreement with the B 2p DOS. It is considered that the high-energy satellite peaks are due to less than four-coordinated B atoms such as have dangling bonds and defects in *w*-BN. In the B K–V x-ray emission spectra of *h*-BN, the synthesizing π and σ sub-bands of B 2p DOS could explain the polarized emission spectra very well.

INTRODUCTION

Boron nitride (BN) is similar to carbon materials such as graphite and diamond in many respects. BN has similar crystal structures to those of carbon. The crystal structures of BN are classified as cubic (*c*-BN), wurtzite (*w*-BN), hexagonal (*h*-BN) and rhombohedral (*r*-BN). Both *c*- and *w*-BN are sp^3-bonded phases in which B atoms combine with neighboring N atoms in four-coordination.[1] The *h*- and *r*-BN are sp^2-bonded phases in which B atoms combine with neighboring N atoms in three-coordination.[1] *h*-BN has a layered graphite-like structure with planar six-membered rings of alternating B and N atoms stacked in an ABAB fashion. BN is more chemically and thermally stable than carbon materials. For instance, carbon materials begin to be oxidized at about 600 °C whereas BN resists oxidation even at elevated temperatures up to about 900 °C.[2] Furthermore, carbon materials react easily with carbide-forming metals such as ferrous alloys whereas BN is non-reactive with these metals.[1] Typical examples of practical uses of *h*-BN are as high-temperature solid lubricants, heating crucibles, microwave guide tubes and high-temperature insulators.[3] The technical use of *c*-BN is mainly in cutting tools because of its extreme hardness. Since *c*-BN and diamond have low densities, extreme hardnesses, large thermal conductivities, wide band gaps and large resistivities,[4] both have been found to be useful for many applications. For example, they are excellent materials for cutting tool coatings and corrosion barriers because of their high hardnesses and chemical resistance, and for insulating and heat sink films of semiconductors because of their large thermal conductivities and resistivities.[5] The advantage of *c*-BN is that it can be especially used to machine steel materials whereas diamond is not suitable. Moreover, the possibility of use as a wide band gap semiconductor is attractive. In particular, *c*-BN can be doped both p-and n-type whereas diamond can only be doped p-type.[6,7] In addition, Mishima[8] has reported the manufacture from doped *c*-BN crystals of an ultraviolet-emitting diode that functions up to 677 °C.

We have previously studied the B K–V x-ray emission spectra of BNs by using electron probe micro-analysis (EPMA), and discussed the electronic structure and the chemical state in order to investigate the formation process and the microstructure of BNs.[9–11] B K–V x-ray emission spectra which are generated from the electronic transition from the 2p to the 1s state due to the dipole selection rule should reflect the valence state of BNs. Hence measuring x-ray emission spectra is a very useful approach for studying the chemical states and crystal structures of BNs. In general, the interpretation of x-ray spectra is based on the comparison of the measured spectra with those of known materials. X-ray spectroscopy is expected to be a more powerful tool when the theoretical support is available. We have calculated C K–V x-ray emission spectra of carbons and applied them to the structural analysis of mechanically milled graphite by using an MO calculation method.[12] The discrete-variational (DV)-Xα method originally written by Adachi and co-workers[13–16] was used for the MO calculation, which is based on the Hartree–Fock–Slater method. The DV-Xα method is applicable to both BNs and carbons.

* Correspondence to: T. Kaneyoshi, Hyogo Prefectural Institute of Industrial Research, 3-1-1, Kouto, Kamigori-cho, Ako-gun, Hyogo 678-1205, Japan.
E-mail address: tkane@hyogo-kg.go.jp

CCC 0049–8246/99/060497–06 $17.50

Received 7 May 1999
Accepted 29 June 1999

In this work, B K–V x-ray emission spectra of various types of BNs were calculated by using the DV-Xα method. The assignment and polarization of B K–V x-ray emission spectra were studied by theoretical calculation.

CALCULATIONS

We applied the method of Manne[17] and Urch[18] and used the DV-Xα MO method to calculate the B K–V x-ray emission spectra, which reflect the density of states (DOS) of B 2p. The calculation procedure of the spectra is as follows.

The kth molecular orbital $\phi_k(\mathbf{r}_1) = \Sigma(i)c_{ik}\chi_i(\mathbf{r}_1)$ is obtained by solving the Schrödinger equation in the one-electron approximation:

$$h(\mathbf{r}_1)\phi_k(\mathbf{r}_1) = \varepsilon_k\phi_k(\mathbf{r}_1) \tag{1}$$

where χ_i, c_{ik} and ε_k are atomic orbital, MO coefficient, and inherent electronic energy, respectively. Here the Schrödinger equation is given by

$$h(\mathbf{r}_1)\sum(j)c_{jk}\chi_j(\mathbf{r}_1) = \varepsilon_k\sum(j)c_{jk}\chi_j(\mathbf{r}_1) \tag{2}$$

The x-ray intensity I is given by[19]

$$I \propto \sum(j)|c_{jk}|^2 \tag{3}$$

The calculated B K–V x-ray spectra are obtained by plotting the B 2p DOS against the inherent electronic energy ε_{2p}. Finally, the calculated spectra are broadened by a convolution of Gaussian function for comparison with measured spectra. The σ and π components of 2p DOS were calculated separately by using MO coefficients of the B 2p orbitals; $I_\sigma \propto \Sigma(j)|c_j(2p_x)|^2 = \Sigma(j)|c_j(2p_y)|^2$, and $I_\pi \propto \Sigma(j)|c_{jj}(2p_z)|^2$.

The DV-Xα MO calculations were carried out on a Windows NT machine with an Alpha-chip processor. The atomic orbitals as a basis set used for the calculation were 1s, 2s, $2p_x$ $2p_y$ and $2p_z$ for all atoms in a cluster. The number of sampling points used for numerical integration was 300 for one atom and the Slater's exchange parameter α was 0.7.

Figure 1 shows the model clusters of *h*-, *c*- and *w*-BNs used for the present calculation. The model cluster of *h*-BN was a mono-layer model, because *h*-BN has a layered structure like graphite[12] and the interactions between interlayers are negligible. For the calculation of the x-ray spectra, only the MO components of the central B atom (black atom in Fig. 1) in each cluster model are considered in order to avoid the influence of cluster edge.

EXPERIMENTAL

B K–V x-ray emission spectra of three types (hexagonal, cubic and wurtzite types) of crystalline BNs were measured. The hexagonal (*h*-) and cubic (*c*-) BN powders were commercial products, and the wurtzite BN (*w*-BN) powder was synthesized using the shock-compression method.[20]

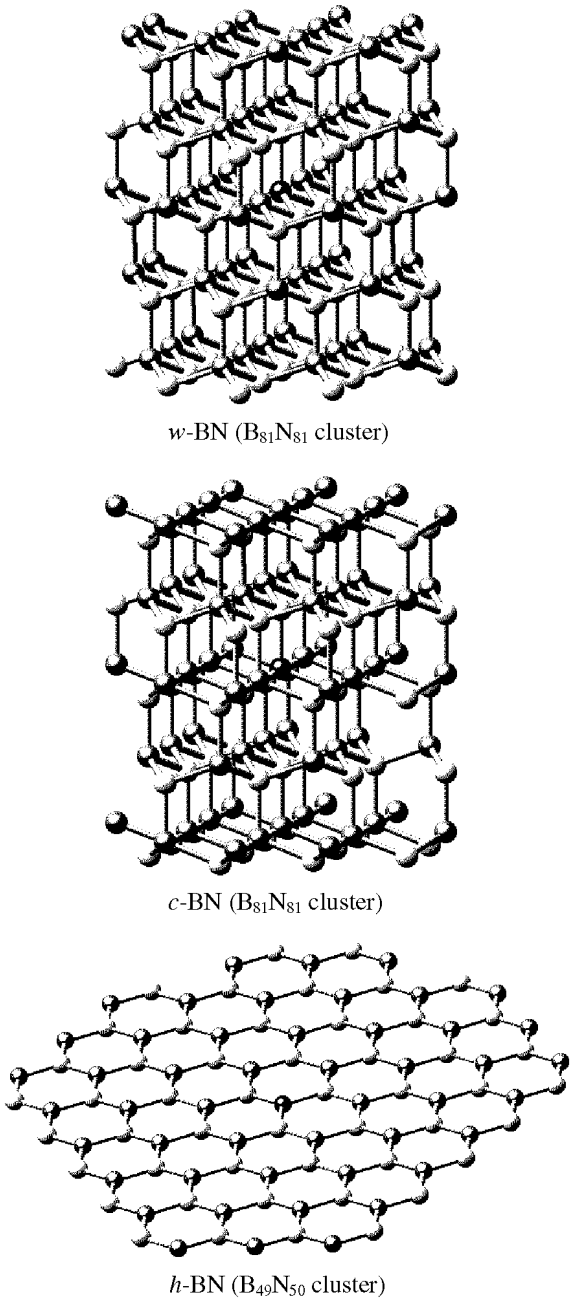

Figure 1. Cluster models of (a) *w*-, (b) *c*- and (c) *h*-BNs used for DV-Xα calculation.

We used EPMA and synchrotron radiation for measuring the x-ray emission spectra. The x-ray emission spectra were measured by EPMA at 15 kV and a beam current of 0.02–0.2 μA. A multilayer pseudo-crystal of lead stearate ($2d = 10$ nm) was used as an analyzer crystal. The x-rays were detected by a gas-flow-type proportional counter and recorded after passing through a pulse-height analyzer in order to prevent overlap of higher order diffraction of other elements in the spectra.

The measurements of the x-ray emission spectra using synchrotron radiation were carried out at the undulator beamline BL-16 of the Photon Factory. Quasi-monochromatic undulator first harmonics were incident

normal to the sample and the photon energies of the first harmonics near the B K-shell threshold were varied by controlling the undulator magnetic gap. We obtained x-ray emission spectra using an entrance-slitless-type grating spectrometer[21] that consisted of a variable-spacing concave grating with an average groove density of 2400 lines mm^{-1} and a gas-flow-type proportional counter.

RESULTS AND DISCUSSION

Figure 2 shows the B K–V x-ray emission spectra of *h*-, *c*- and *w*-BNs measured by using EPMA. The spectra of BNs consist of the main peak at 181 eV and a low-energy satellite at 170 eV. Triangular *h*-BN can be distinguished from tetrahedral *c*- and *w*-BNs by using the peak shift of main peaks in the B K–V x-ray emission spectra. However, it is difficult to distinguish *w*-BN from *c*-BN, although there are small differences regarding high-energy satellites and asymmetry of main peaks. Figure 3 shows the B K–V x-ray emission spectra of *h*-, *c*- and *w*-BNs using synchrotron radiation, exited with a 94 mm magnetic gap, at which the most intense high-energy satellites were obtained in *w*- and *h*-BNs, on which the fluorescence-yield absorption spectra at the B K-shell threshold are superimposed. The profiles of the high-energy satellite peaks increase and become clear owing to excitation at the B K-shell threshold. It is found that the high-energy satellite peaks correspond to the absorption spectra. A small broad peak in the spectrum of *c*-BN is considered to be due to elastic scattering of incident undulator first harmonics because the peak shape is similar to the spectral shape of the incident undulator first harmonics. There is a sharp difference among the profiles of the high-energy satellite peaks, so we can distinguish among *c*-, *w*- and *h*-BNs.

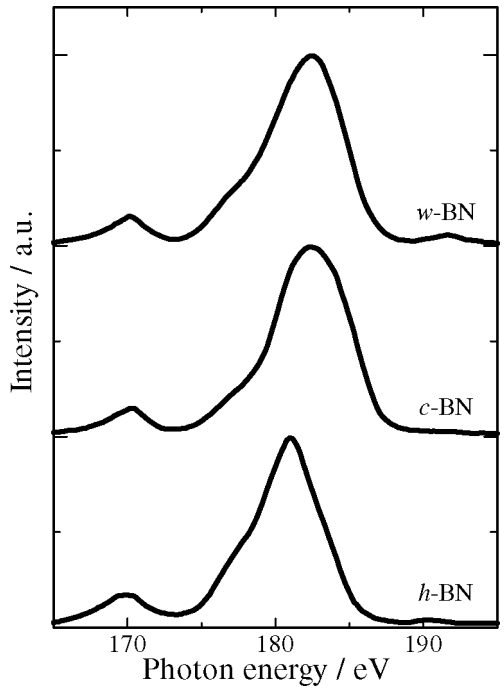

Figure 2. Boron K–V x-ray emission spectra of *h*-, *c*- and *w*-BNs measured by using EPMA.

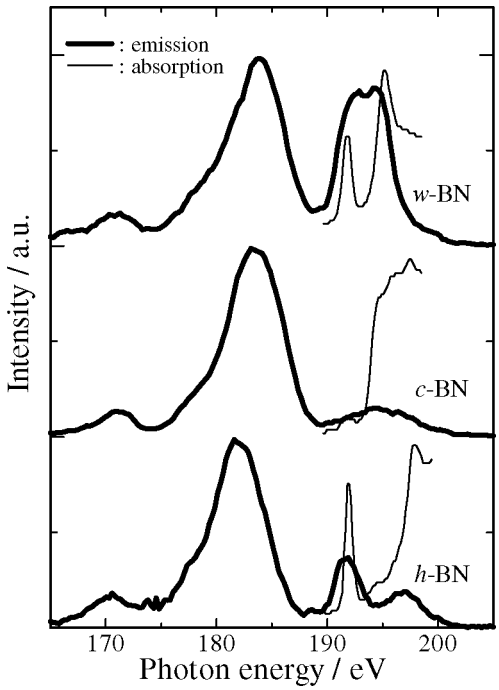

Figure 3. Boron K–V x-ray emission spectra of *h*-, *c*- and *w*-BNs using synchrotron radiation, excited with a 94 mm magnetic gap, superimposed on the fluorescence-yield absorption spectra.

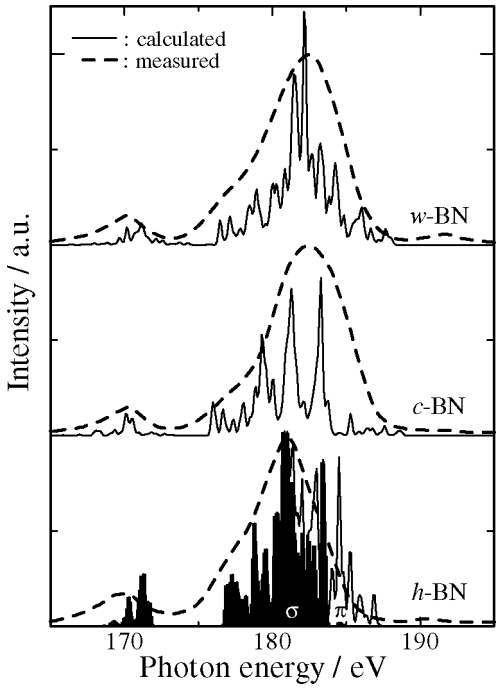

Figure 4. Boron 2p DOS calculated for cluster models of *h*-, *c*- and *w*-BNs shown in Fig. 1 compared with measured spectra.

The DV-Xα method was applied to reproduce the B K–V x-ray emission spectral profiles of *c*-, *w*- and *h*-BNs for the purpose of investigating the assignment of electronic states and applying it to a structural analysis. Figure 4 shows the B 2p DOS calculated for models of *h*-, *c*- and *w*-BNs shown in Fig. 1, compared with measured spectra. The B 2p MO components are broadened by a 0.1 eV width Gaussian. The energy values of the B 2p DOS are relative to the B 1s and added 13 eV for

fitting the measured spectra. In the present work, we did not use the transition-state method based on the Slater transition-state theorem[22,23] or the ΔSCF method,[24] but used the ground-state method for MO calculation. This is because the number of self-consistent field calculations is very large and the calculation becomes very difficult for large cluster. We found that the difference between the ground-state energies and the transition-state energies are approximately constant, because all the valence orbitals have about the same Coulomb energy from the x-ray holes. Therefore, the results of the ground-state method properly reflect the transition-state calculations and the comparison of the results of the ground-state method with the x-ray emission spectra is reasonable. The B 2p DOS of *h*-, *c*- and *w*-BNs are in good agreement with the measured spectra. The π and σ sub-bands originating from the B 2p DOS of *h*-BN are indicated in Fig. 4. In the B 2p DOS of *h*-BN which has a three-coordinate bond, it is observed that π and σ sub-bands are localized. Figure 5 shows molecular orbital levels and orbital components of B and N 1s, 2s and 2p orbitals. It is easily found that the main peaks and low-energy satellite peaks in the B K–V x-ray emission spectra are due to the B 2p hybridized with N 2p and the B 2p hybridized with N 2s, respectively. Figure 6 shows the B 2p DOS of unoccupied orbitals calculated for *h*-, *c*- and *w*-BNs. The dotted and solid lines indicate occupied and unoccupied orbitals, respectively. The ratio of unoccupied and occupied orbitals is arbitrary. The DOS of unoccupied orbitals can be compared with the measured x-ray emission spectra, because the high-energy satellite peaks correspond to the absorption spectra as mentioned above. The high-energy satellite peak in B K–V x-ray emission spectra clearly correspond to the π^* sub-band of the B 2p DOS in *h*-BN. However, the high-energy satellite peak observed in *w*-BN is not agreement with the B 2p DOS. Although the position of the high-energy satellite peak is near that of *h*-BN, the shape of peak is different from that of *h*-BN and existence of *h*-BN is not observed using x-ray diffraction analysis. We considered that the high-energy satellite peak is not due to the four-coordinated B atoms in *w*-BN, but to the less than four-coordinated B atoms, e.g. B atoms in *h*-BN. In the present work, *w*-BN synthesized using the shock-compression method was used for measuring the B K–V x-ray emission spectra as mentioned above. In the shock-compression method, matter was melted and cooled rapidly. Therefore, the grain size became very small and many defects or imperfections were introduced into the matter. Hence it is considered that there are many less than four-coordinated B atoms that have dangling bonds or defects in *w*-BN synthesized using shock-compression method. The B 2p DOS of a dangling bond in *w*-BN located at the corner of *w*-BN is indicated in Fig. 6. The high-energy satellite peak is in good agreement with the unoccupied orbitals of the B 2p DOS of dangling bonds. Therefore, it is concluded that the high-energy satellite peak observed in *w*-BN is due to unoccupied orbitals of less than four-coordinated B atoms such as having dangling bonds or defects.

Mansour and co-workers[25,26] observed polarization effect and suggested a theoretical equation for the contribution of σ and π valence electrons to the B K–V x-ray emission spectrum in *h*-BN. The characteristic x-rays

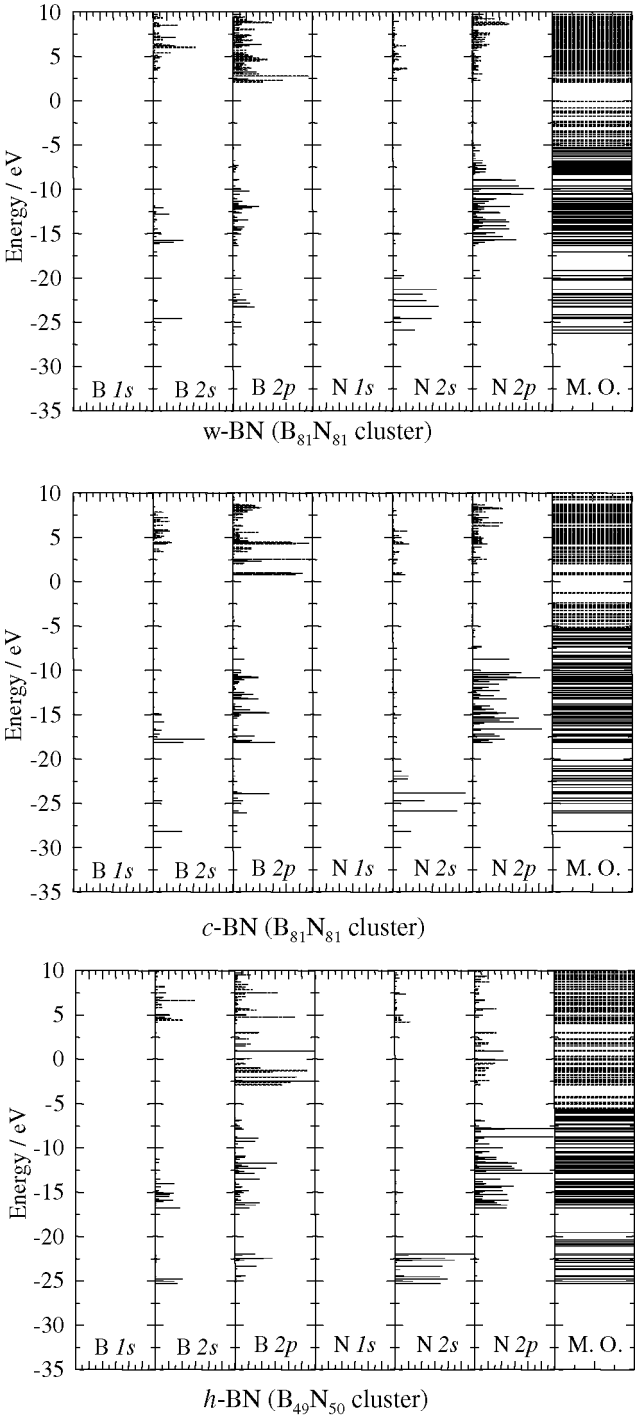

Figure 5. Molecular orbital levels and orbital components of B and N 1s, 2s and 2p orbitals.

are emitted perpendicular to the orbital direction. The x-ray intensity as a function of the take-off angle θ is given by a linear combination of σ and π emission intensities:

$$I(E,\theta) = I\sigma(E)[(1+\cos^2\theta)/2] + I\pi(E)\sin^2\theta \qquad (4)$$

where $I\sigma(E)$ and $I\pi(E)$ are the x-ray intensities of σ and π orbitals, respectively. Hence $I(E,\theta)$ changes with the take-off angle. Figure 7 shows the B 2p DOS calculated for *h*-BN by synthesizing the π, σ and π^* sub-bands according to the polarized emission equation [Eq (4)]. The low-energy satellite peak (mainly B 2pσ) decreases and

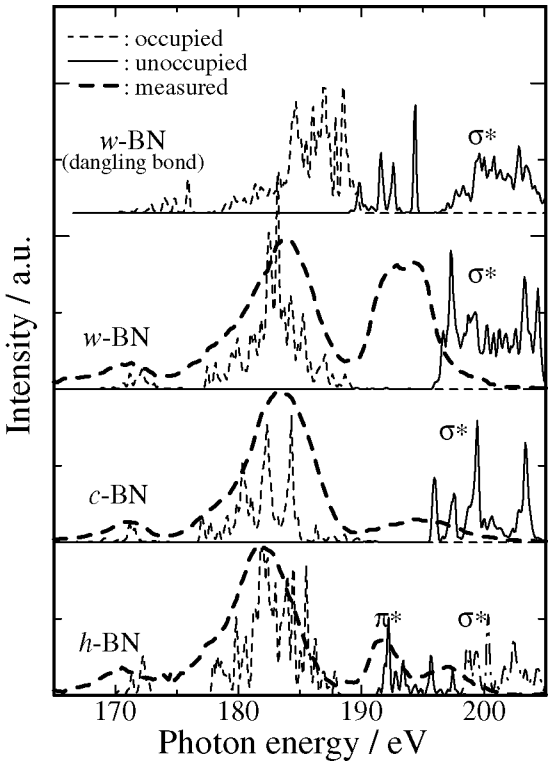

Figure 6. Boron 2p DOS of unoccupied orbitals and calculated for *h*-, *c*- and *w*-BNs.

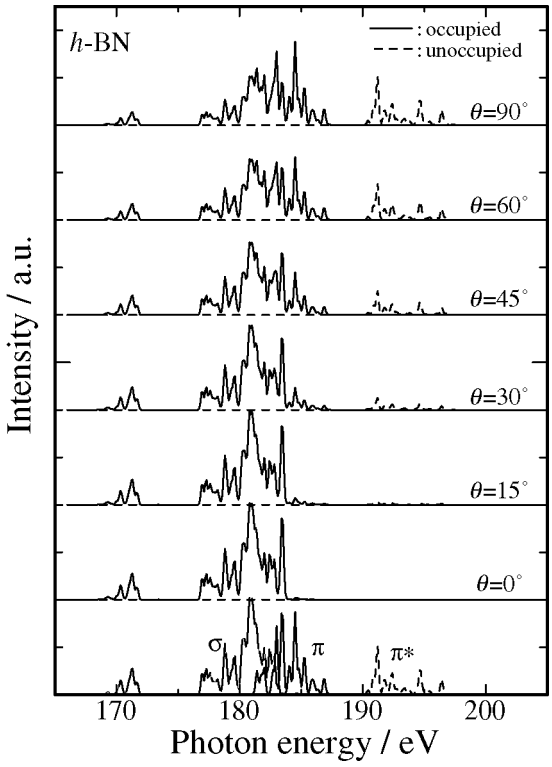

Figure 7. Boron 2p DOS calculated for *h*-BN by synthesizing the π, σ and π^* sub-bands according to the polarized emission equation [Eqn (4)].

the high-energy satellite peak (mainly B 2pπ^*) increases with increasing take-off angle. This result of calculation is in excellent agreement with those of the B K–V x-ray emission spectra measured by Mansour and Schnatterty.[25] This suggests that the polarization of spectra can be discussed in detail by using the DV-Xα MO calculation.

In summary, B K–V x-ray spectral profiles of *h*-, *w*- and *c*-BNs could be reproduced by calculating the B 2p DOS with the DV-Xα method. The assignment of each peak of the B K–V x-ray emission spectra could be explained. Furthermore, the synthesized π and σ sub-bands of B 2p DOS explained the polarized emission spectra very well. Based on these results, the structures of BN systems are expected to be analyzed by x-ray emission spectroscopy. Especially structural analysis using polarized emission spectra is expected to be advanced.

CONCLUSIONS

The B K–V x-ray emission spectra of *h*-, *w*- and *c*-BNs were studied with the DV-Xα MO calculation method. The calculated B 2p DOS reproduced the measured spectral profiles and the peaks of the B K–V x-ray emission spectra were assigned. It was found that the main peak and the low-energy satellite in the B K–V x-ray emission spectra were due to the B 2p and the B 2p hybridized with N 2s, respectively. The high-energy satellite corresponded to the π^* sub-band of the B 2p DOS in *h*-BN. In *w*-BN, the high-energy satellite was due to the B 2pσ^* of B atoms which have dangling bonds and defects. The polarized spectra were reproduced by synthesizing from the π and σ sub-bands. It is suggested that the polarization of spectra could be discussed and applied to structural analysis in detail by using the DV-Xα MO calculation method.

REFERENCES

1. T. A. Friedmann, P. B. Mirkarimi, D. L. Medlin, K. F. McCarty, E. J. Klaus, D. R. Boehme, H. A. Johnsen, M. J. Mills, D. K. Ottesen and J. C. Barbour, *J. Appl. Phys.* **76**, 3088 (1994).
2. S. Komatsu, T. Yoshida and K. Akashi, in *Proceedings of the 9th Symposium on ISIAT '85*, edited by T. Takagi, Tokyo, p. 421. The Discussion Group of Ion Engineering, Tokyo (1985).
3. K. Sugiyama and H. Itoh, *Mater. Sci. Forum*, **54–55**, 141 (1990).
4. H. Saitoh and Y. Ichinose, *Bull. Jpn. Inst. Met.* **27**, 720 (1988).
5. T. Ichiki, T. Momose and T. Yoshida, *J. Appl. Phys.* **75**, 1330 (1994).
6. R. M. Chrenko, *Phys. Rev. B* **7**, 4560 (1973).
7. D. K. Ferry, *Phys. Rev. B* **12**, 2361 (1975).
8. O. Mishima, *Mater. Sci. Forum* **54–55**, 313 (1990).
9. H. Kohzuki and M. Motoyama, *Adv. X-Ray Chem. Anal. Jpn.* **23**, 43 (1992).
10. H. Kohzuki and M. Motoyama, *J. Jpn. Inst. Met.* **56**, 565 (1992).
11. H. Kohzuki and M. Motoyama, *J. Jpn. Inst. Met.* **56**, 572 (1992).
12. T. Kaneyoshi, Y. Kowada, T. Tanaka, J. Kawa and M. Motoyama, *Spectrochim. Acta, Part B* **54**, 189 (1999).
13. D. E. Ellis and G. S. Painter, *Phys. Rev. B* **2**, 2887 (1970).
14. A. Rosén, D. E. Ellis, H. Adachi and F. W. Averill, *J. Chem. Phys.* **65**, 3629 (1976).

15. H. Adachi, M. Tsukada and C. Saito, *J. Phys. Soc. Jpn.* **45**, 875 (1978).
16. C. Saito, M. Tsukada and H. Adachi, *J. Phys. Soc. Jpn.* **45**, 1333 (1978).
17. R. Manne, *J. Chem. Phys.* **52**, 5733 (1970).
18. D. S. Urch, *J. Phys. C* **3**, 1275 (1970).
19. J. Kawai and K. Hashimoto, *Adv. X-Ray Chem. Anal. Jpn.* **49**, 1944 (1992).
20. A. K. Lam, R. M. Wentzcovitch and M. L. Cohen, in *Synthesis and Properties of Boron Nitride*, edited by J. J. Pouch and S. A. Alterovitz, p. 165. Trans Tech, Aedermannsdorf (1990).
21. Y. Muramatsu, M. Oshima, T. Shoji and H. Kato, *Rev. Sci. Instrum.* **63**, 5597 (1992).
22. J. C. Slater, *Quantum Theory of Molecular and Solids, the Self-Consistent Field for Molecular and Solids*, Vol. 4 McGraw-Hill, New York (1974).
23. H. Adachi and K. Taniguchi, *J. Phys. Soc. Jpn.* **49**, 1944 (1980).
24. H. Agren and A. Flores-Riveros, *J. Electron Spectrosc. Relat. Phenom.* **56**, 259 (1991).
25. A. Mansour and S. E. Schnatterly, *Phys. Rev. B* **36**, 9234 (1987).
26. A. Mansour, S. E. Schnatterly and R. D. Carson, *Phys. Rev. B* **31**, 6521 (1985).

